Modelling and Control of Erosion of a Choke in a Gas Lifted Well Network

Project Thesis

Author:
Joachim Ågotnes

Supervisor:
Johannes Jäschke

Co-supervisor:
Jose Matias

Norwegian University of Science and Technology

December 18, 2019

Abstract

This project aims to model erosion of a choke in a gas lifted well network with the use of data driven models to be able to do better maintenance optimization in the oil and gas industry. Modelling of erosion is important to determine when subsea equipment fails, which is a big expense for the oil and gas industry. However, modelling erosion is very complex as the flow in the pipelines consists of multiple phases with different flow regimes. Much research has been done on this field, but most of the previous models are inaccurate. Firstly, a model for three separate wells combined with a riser was created. This was done by using an existing model for a gas lifted well network and including an erosion model into the model of the gas lifted well network. Secondly, a model predictive control (MPC) was made to control the erosion in each well with the goal of maximizing oil production while keeping the erosion of the choke in each well below a certain threshold. The response from the MPC gives the indication that this type of controller can be used to control erosion. Lastly, data driven models such as ARX, ARMAX and OE models were created to make accurate models for erosion. The results from using data driven models show that all of the models can be used to model erosion. Further research should look into applying the data driven models into the controller and then test it with an experiment to further validate that it is possible to use data driven models for control purposes of erosion.

Contents

List of Symbols

α	Characteristic impact angle	rad
Δu_{max}	Maximum change in input	$\mathrm{kg\,s^{-1}}$
$\dot{m}_p$	Sand rate	$\mathrm{kg\,s^{-1}}$
γ	Relation between particle diameter and diameter of choke	-
γ_c	Relative critical particle diameter	-
μ	Dynamic viscosity	$\mathrm{kg\,m^{-1}\,s^{-1}}$
ρ	Density	$\mathrm{kg\,m^{-3}}$
ρ_a	Density of the gas in the annulus	$\mathrm{kg\,m^{-3}}$
ρ_o	Density of the oil	$\mathrm{kg\,m^{-3}}$
ρ_p	Density of sand particles	$\mathrm{kg\,m^{-3}}$
ρ_s	Weighting for slack variable	-
ρ_w	Density of the mixture in the tubing	$\mathrm{kg\,m^{-3}}$
A	Dimensionless constant	-
A_g	Area of the annulus	$\mathrm{m^2}$
A_g	Effective gallery area	$\mathrm{m^2}$
A_p	Area of pipe	$\mathrm{m^2}$
A_r	Cross-sectional area of piping over the injection point	$\mathrm{m^2}$
A_t	Area exposed to erosion	$\mathrm{m^2}$
A_w	Cross-sectional area of piping under the injection point	$\mathrm{m^2}$
C_1	Model geometry factor	-
C_{iv}	Valve constant for the injection valve	-
C_{pc}	Valve constant for the production valve	-
C_{unit}	Unit conversion factor	$\mathrm{mm\,m^{-1}}$
D	Length from cage and choke body	m
d_p	Sand particle diameter	m
E	Erosion	mm
ER	Erosion rate	$\mathrm{mm\,yr^{-1}}$
G	Particle size correction factor	-
g	Gravitational constant	$\mathrm{m\,s^{-2}}$

GF	Geometry factor	-
GOR	Gas-oil ratio	-
H	Height of gallery	m
H_r	Height of tubing under the injection point	m
H_w	Height of tubing above the injection point	m
K	Material erosion constant	-
L_a	Length of annulus	m
L_w	Length of piping over the injection point	m
L_{bh}	Length of piping under the injection point	m
M	Weighting matrix for collocation points	-
m_{ga}	Mass of gas in the annulus	kg
m_{gt}	Mass of gas in the tubing	kg
m_{ot}	Mass of oil in the tubing	kg
Mm_g	Molar mass of the gas	$\mathrm{g\,mol^{-1}}$
MSE	Mean square error	-
N	Number of observations	-
n	Velocity exponent	-
n_a	Number of previous values of the outputs	-
n_b	Number of previous values of the inputs	-
n_c	Number of previous values of the errors	-
n_f	Number of previous values of the noise free outputs	-
n_k	Dead time	-
n_p	Number of parameters	-
$NRMSE$	Normalized root mean square error	-
p	Pressure	bar
p_a	Pressure in the annulus	Pa
p_{bh}	Pressure at the bottom hole	Pa
p_m	Pressure in the manifold	Pa
p_r	Pressure in the reservoir	Pa
p_{wh}	Pressure in the wellhead	Pa

p_{wi}	Pressure at the injection point	Pa
PI	Reservoir productivity index	-
Q	Volumetric flow	$\mathrm{m^3\,s^{-1}}$
R	Gas constant	$\mathrm{J\,K^{-1}\,mol^{-1}}$
r	Radius of curvature	m
$R_{\Delta u}$	Weighting matrix for regularization term in MPC	-
$s(t)$	Slack term in MPC	-
T	Temperature	K
T_a	Temperature in the annulus	K
t_m	Input horizon	-
t_p	Prediction horizon	-
T_w	Temperature in the tubing	K
U_p	Characteristic impact velocity	$\mathrm{m\,s^{-1}}$
u_{max}	Maximum value of the input	$\mathrm{kg\,s^{-1}}$
u_{min}	Minimum value of the input	$\mathrm{kg\,s^{-1}}$
V	Superficial velocity	$\mathrm{m\,s^{-1}}$
V_a	Volume of the annulus	$\mathrm{m^3}$
w	Mass rate	$\mathrm{kg\,s^{-1}}$
w_{gl}	Gas lift injection rate	$\mathrm{kg\,s^{-1}}$
w_{iv}	Mass flow rate of gas from the annulus to the tubing	$\mathrm{kg\,s^{-1}}$
w_{pc}	Mass flow rate of through the production choke	$\mathrm{kg\,s^{-1}}$
w_{pg}	Mass flow rate of produced gas	$\mathrm{kg\,s^{-1}}$
w_{po}	Mass flow rate of produced oil	$\mathrm{kg\,s^{-1}}$
w_{rg}	Mass flow rate of gas from the reservoir	$\mathrm{kg\,s^{-1}}$
w_{ro}	Mass flow rate of oil from the reservoir	$\mathrm{kg\,s^{-1}}$

1 Introduction

Erosion is a known problem in the oil and gas industry as it requires the industry to do maintenance and production stops. Having accurate and precise models of erosion would open for control of erosion to reduce production stops as well as maintenance costs.

There has previously been work done on modelling erosion and especially at The University of Tulsa, where Chen made a procedure for estimating erosion in elbows in multiphase flows [1] and Mazumder made a mechanistic model to predict sand erosion in multiphase flow in elbows [2]. Most of the previous work does not look at erosion in chokes, but DNV-GL wrote a recommended practise for erosion in chokes and valves [3]. By having accurate predictions of erosion, it is possible to save maintenance cost by including the models in a control framework such as a model predictive control (MPC) to control the erosion rate. It is thus possible to do maintenance optimization with the goal of saving maintenance costs.

Although there has been much effort to try to model erosion, the resulting models are inaccurate due to the complexity of the problem. The erosion rate is a function of many different parameters such as the bulk properties, particle properties and target material properties. The current models are mostly created with partially calculations based on fluid dynamics and experimental results. By doing system identification with data driven models it is possible to make models solely based on experimental data. These types of models utilizes weightings calculated from the experimental data together with previous recorded data to predict the erosion. There is a whole family of data driven models, but in this work the focus will be on ARX, ARMAX and OE models.

This project thesis consists of several parts, where the first one is modelling the erosion of a choke within a gas lift well system with 3 wells with different parameters. The second part will be on creating a model predictive controller to control the system with the model found in the first part with the purpose to maximize production of oil while keeping the erosion of the choke in each well below a threshold. The last part will be on system identification, where the purpose is to identify a data driven model and parameters related to the model for each well, which again can be used to predict the erosion in the first part.

2 Erosion

Subsea equipment is prone to both chemical and mechanical wear. There are several mechanisms connected to both chemical and mechanical wear such as corrosion, sand erosion and corrosion-erosion. Previous work show that erosion due to sand particles is a big problem related to failure in subsea equipment [4]. Oil and gas wells produce sand to some extent. Sand screens can be used to prevent some of the sand, although it is not enough to prevent erosion due to sand particles. This thesis will only be looking at sand erosion, as sand erosion is one of the biggest issues related to corrosion and erosion in subsea equipment.

In Fig. 1 an example of how erosion of ductile materials such as most metals happen is shown. In (a) the particle and the ductile material is shown before impact. The particle will hit the ductile material and form a crater and material will be accumulated such as shown in (b). When another particle hits the accumulated material, it will transfer some of its kinetic energy and remove some

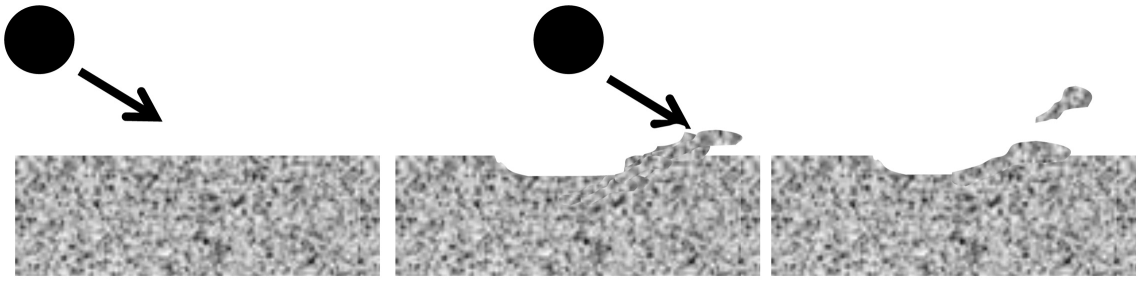

Figure 1: Visual representation showing erosion of ductile materials [4].

of the ductile material as shown in (b) and (c). As this happens multiple times, the indent caused by the particles will become larger.

Sand erosion is a function of many parameters. When the particles hit a target material, some of its kinetic energy will be transferred to the target material, thus making the target material subject to erosion. The size of the sand particles will have an effect on the erosion rate as the bigger the particles are, the more kinetic energy the particles will have and more energy is transferred. The mass flow rate of the sand particles will have a significant impact as having a higher mass flow rate of sand particles will cause more particles to hit the target material, causing a higher grade of erosion. The shape of the particles will have an impact as round particles cause less erosion than particles with edges. The angle that the sand particles hit the valve will also have an impact. Parameters related to the sand particles such as density, size and hardness will also impact the erosion rate. Another factor that should not be forgotten about is the bulk properties. The gas/liquid content, the bulk velocity, the viscosity and the density of the fluid will all impact the erosion rate greatly [4].

3 Modelling Erosion in a Gas Lifted Well Network

Simulating erosion can be valuable method to test models instead of having to do experiments as experiments are time consuming and often costly. To create a model, good prior knowledge about the system is required. By including an erosion model in an existing model for a gas lifted well system, it is possible to simulate the erosion rate of a choke in the gas lift. The modelling is thus divided in two, where the first part describes the gas lift model and the second part describes the erosion model for a choke.

3.1 Gas Lift Model

Gas lift is used in wells where the pressure of the reservoir is not enough to drive the oil to the surface at a sufficient level. By injecting gas into the well through the annulus, the mixture density of the fluid in the tubing decreases. Thus there is a decrease in the hydrostatic pressure in the bottom hole. This makes the pressure difference larger and the flow from the reservoir is increased. The model used to describe the gas lifted well system is based on the model as Krishnamoorthy used for real-time optimization applied to a gas lifted well system [5]. The model equations are valid for all

of the wells in the gas lifted well system which consists of three wells, but to simplify, the model equations for one well is shown. A simplified figure of the gas lift system and the parameters used in the modelling is shown in Fig. 2.

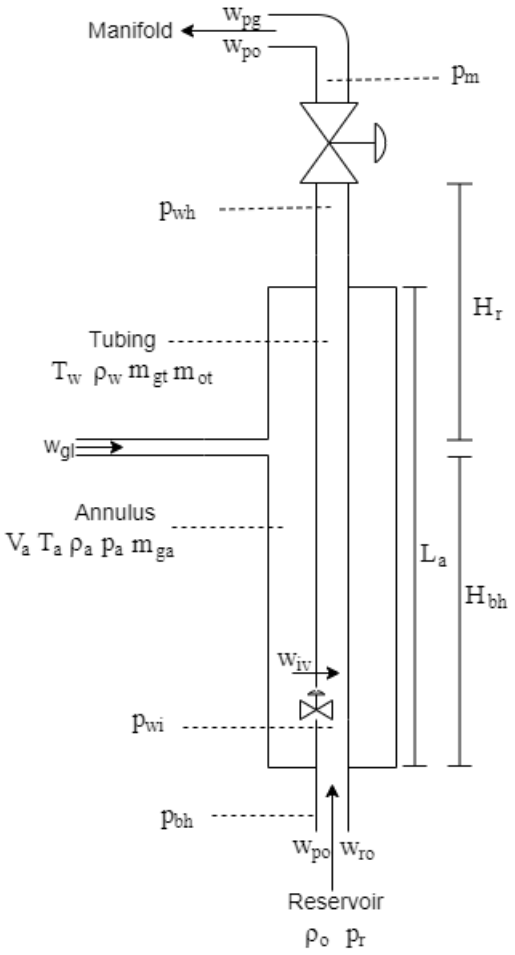

Figure 2: Simplified figure of the gas lift.

The mass balance for a well is described by the difference between the mass flow rates in and out of the annulus and tubing for both the gas and the oil.

$$\dot{m}_{ga} = w_{gl} - w_{iv} \tag{1a}$$
$$\dot{m}_{gt} = w_{iv} - w_{pg} + w_{rg} \tag{1b}$$
$$\dot{m}_{ot} = w_{ro} - w_{po} \tag{1c}$$

Where $\dot{m}_{ga}$ describes the change of mass in the annulus with respect to time, $\dot{m}_{gt}$ describes the change of mass in the tubing with respect to time and $\dot{m}_{ot}$ describes the change of mass of oil in the tubing with respect to time. The gas lift injection rate is described by w_{gl} and w_{iv} denotes the mass flow rate of gas from the annulus and to the tubing. w_{pg} describes the mass flow rate of produced

gas while w_{po} is the mass flow rate of produced oil. w_{rg} describes the mass flow rate of gas from the reservoir wile w_{ro} is the mass flow rate of oil from the reservoir [5].

To get the density of the gas located in the annulus, ρ_a, the ideal gas law is used. The density of the mixture of the oil and gas in the tubing, ρ_w, is given by the total mass of gas and oil in the tubing after the injection point divided by the total volume of the piping after the injection point.

$$\rho_a = \frac{Mm_g \cdot p_a}{T_a \cdot R} \tag{2a}$$

$$\rho_w = \frac{m_{gt} + m_{ot} - \rho_o \cdot L_{bh} \cdot A_{bh}}{L_w \cdot A_w} \tag{2b}$$

Mm_g describes the molar mass of the gas, while R denotes the gas constant. p_a and T_a are the pressure and the temperature in the annulus, respectively. The density of the oil is given by ρ_o. L_{bh}, A_{bh}, L_w and A_w describes the length and cross-sectional area of the piping in the well before and after the injection point for the gas lift system.

To get the pressures in the annulus, p_a, and the pressure in the wellhead, the ideal gas law is once again used. The pressure in the injection point, p_{wi}, and the pressure in the bottom hole, p_{bh}, are calculated from the hydrostatic pressure.

$$p_a = m_{ga}\left[\frac{T_a \cdot R}{V_a \cdot Mm_g} + \frac{g \cdot L_a}{L_a \cdot A_a}\right] \tag{3a}$$

$$p_{wh} = \frac{T_w \cdot R}{Mm_g}\left[\frac{m_{gt}}{L_w \cdot A_w + L_{bh} \cdot A_{bh} - \frac{m_{ot}}{\rho_o}}\right] \tag{3b}$$

$$p_{wi} = p_{wh} + \frac{g}{A_w \cdot L_w}(m_{ot} + m_{gt} - \rho_o \cdot L_{bh} \cdot A_{bh}) \cdot H_w \tag{3c}$$

$$p_{bh} = p_{wi} + \rho_w \cdot g \cdot H_{bh} \tag{3d}$$

Where m_{ga} is the mass of gas in the annulus, V_a is the volume of the annulus, g is the gravitational constant and A_a is the cross-sectional area of the annulus. The total length of the annulus is given by L_a. The temperature inside of the tubing is given by T_w. m_{gt} and m_{ot} describes the mass of gas and oil in the tubing. H_w describes the height of the tubing above the injection point for the gas lift while H_{bh} is the height of the tubing after the injection point for the gas lift [5].

The mass flow rate from the annulus to the tubing, w_{iw}, and the total production mass flow rate, w_{pc}, can be calculated by valve equations. The produced oil and gas, w_{pg} and w_{po} are calculated from mass ratios of oil and gas in the tubing and the total production. The mass flow rate of oil, w_{ro}, is given by the difference in pressure of the reservoir and bottom hole pressure. The mass flow rate of gas from the reservoir, w_{rg}, is calculated from the mass flow of gas from the reservoir and

the *GOR*.

$$w_{iv} = C_{iv} \cdot \sqrt{\rho_a \max\left(0, p_{ai} - p_{wi}\right)} \tag{4a}$$
$$w_{pc} = C_{pc} \cdot \sqrt{\rho_w \max\left(0, p_{wh} - p_m\right)} \tag{4b}$$
$$w_{pg} = w_{pc} \cdot \frac{m_{gt}}{m_{gt} + m_{ot}} \tag{4c}$$
$$w_{po} = w_{pc} \cdot \frac{m_{ot}}{m_{gt} + m_{ot}} \tag{4d}$$
$$w_{ro} = PI \cdot (p_r - p_{bh}) \tag{4e}$$
$$w_{rg} = GOR \cdot w_{ro} \tag{4f}$$

Where w_{pc} represents the mass flow rate through the production choke. C_{iv} and C_{pc} are valve constants for the injection valve and the valve that controls the production. p_m and p_r describes the pressure in the manifold and the pressure of the reservoir, respectively [5]. The reservoir productivity index is given by *PI* and is used to describe the reservoirs potential to produce oil and gas. The gas-oil ratio is denoted by *GOR*. Both the *PI* and the *GOR* are model parameters.

3.2 Erosion Model

The erosion model is based on a choke model from DNV-GL which gives the erosion rate with an uncertainty of a factor of at least ± 3 [3]. Chokes come in many different forms and geometric layouts which makes it difficult to find a generic model. To get an accurate measurement of the erosion rate, CFD is usually used in each specific case [3].

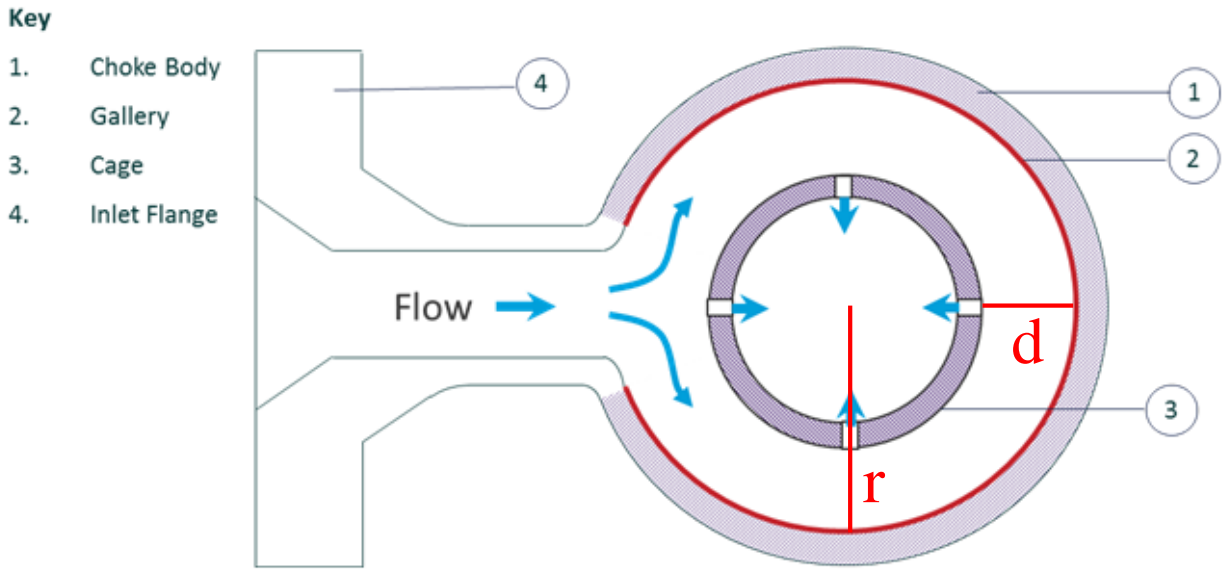

Figure 3: Description of a choke gallery [3].

An example of an angle style choke is shown in Fig. 3. These types of chokes are prone to erosion especially if the choke body is much smaller than the piping or the gallery of the choke is small [3].

The characteristic impact velocity of the sand particles is given by:

$$U_p = \frac{3}{4}\frac{Q_m}{A_g} \tag{5}$$

With the effective gallery area given as $A_g = 2 \cdot H \cdot D$ where H is the height of the choke gallery and D is the length from the cage and the choke body. The mixed volumetric flow rate given by $Q_m = Q_{po} + Q_{pg}$.

The characteristic impact angle, α, which is the angle that the sand particles hit the choke in radians is given by:

$$\alpha = arctan(\frac{1}{\sqrt{2 \cdot r}}) \tag{6}$$

Where r is the radius of curvature which in the case of a choke is described by the radius of the choke gallery and is also shown in Fig. 3.

$F(\alpha)$ is used to correct the erosion rate for the impact angle and for ductile materials it is given by:

$$F(\alpha) = 0.6 \cdot [sin(\alpha) + 7.2(sin(\alpha) - sin^2(\alpha))]^{0.6} \cdot [1 - exp(-20 \cdot \alpha)] \tag{7}$$

The relation between the critical particle diameter, $d_{p,c}$ and the length from the cage and choke body, D, is given by:

$$\frac{d_{p,c}}{D} = \gamma_c = \begin{cases} \frac{\rho_m}{\rho_p[1.88 \cdot ln(A) - 6.04]}, & \gamma_c < 0.1 \\ 0.1, & 0 \geq \gamma_c > 0.1 \end{cases} \tag{8}$$

Where ρ_m is the density of the mixture, ρ_p is the density of the particles and A is a dimensionless constant given by:

$$A = \frac{\rho_m^2 \cdot tan(\alpha) \cdot U_p \cdot D}{\rho_p \cdot \mu_m} \tag{9}$$

The dynamic viscosity of the mixture, μ_m is calculated by the procedure given in Appendix C under the assumptions of ideal gas.

The relation between the sand particle diameter and the length from the cage and the choke body is given by:

$$\gamma = \frac{d_p}{D} \tag{10}$$

Where d_p is the diameter of the sand particles.

The particle size correction factor is given by:

$$G = \begin{cases} \frac{\gamma}{\gamma_c}, & \gamma < \gamma_c \\ 1, & \gamma \geq \gamma_c \end{cases} \tag{11}$$

The area exposed to erosion, A_t, is given by:

$$A_t = \frac{A_{pipe}}{sin(\alpha)} \tag{12}$$

Where A_{pipe} is the area of the pipe.

The erosion rate, ER, is given by:

$$ER = \frac{dE}{dt} = \frac{K \cdot F(\alpha) \cdot U_p^n}{\rho_t \cdot A_t} \cdot G \cdot C_1 \cdot GF \cdot \dot{m}_p \cdot C_{unit} \tag{13}$$

Where E is the erosion in mm, K is the material erosion constant, n is the velocity exponent, ρ_t is the density of the material, C_1 is a model geometry factor, GF is a geometry factor, $\dot{m}_p$ is the mass sand rate and C_{unit} is a unit conversion factor. The impact velocity, U_p, is given by Eq. (5). The erosion rate describes how many millimeters of the choke that will erode per second ($\mathrm{mm\,s^{-1}}$). The variable in the model is U_p, while K, $F(\alpha)$, n, ρ_t, A_t, G, C_1, GF and $\dot{m}_p$ are model parameters.

4 Model Predictive Control

By using a model predictive control (MPC) framework, it is possible to control a system such as the erosion rates of a choke in a gas lift well network. These types of controllers are being used to great extent due to the capabilities of handling non-linear constraints and disturbances [6].

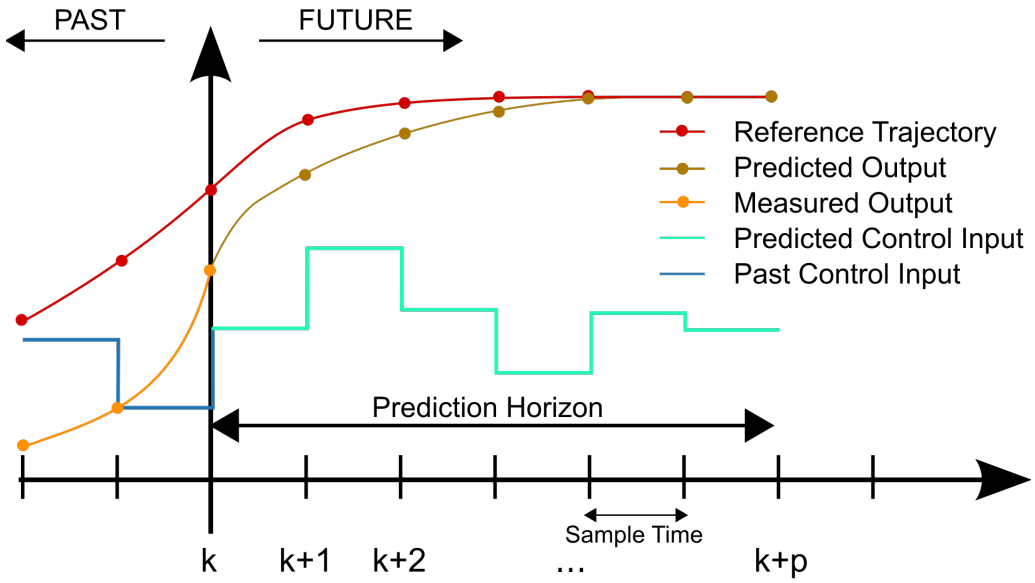

Figure 4: Description of a model predictive controller [7].

Figure 4 shows a schematic of an MPC controller. At every time step, the MPC controller will make a prediction to find the optimal trajectory for the inputs based on the current state of the system. The prediction horizon can be divided into the input horizon and the output horizon. The input horizon describes the time period where the controller can change the inputs, while between the input and output horizon it must keep the input constant. This is used to prevent too aggressive input moves. At each time step after calculating the set of optimal inputs, the controller will apply the first control move and then reoptimize.

The objective function is the goal of the controller, which it desires at every time. There exists several types of objectives for the MPC such as economic controllers or set point controllers where the ladder is the objective of Fig. 4 which in this case is to keep as close to the reference trajectory as possible. Often the objective can be to maximize profit or reduce costs. The following objective function, which is minimized, is used to describe an economic MPC with a regularization term:

$$\Psi = \int_0^{t_p} \left(-cost + \frac{1}{2} \Delta u(t)^T R_{\Delta u} \Delta u(t) \right) dt \tag{14}$$

Where t_p is the prediction horizon. The second term describes a regularization term on the change in inputs, Δu. This means that the controller wants to minimize the change of inputs. $R_{\Delta u}$ is a tuning parameter which describes the weighting of the regularization term on the original objective function.

The system consists of both algebraic and differential equations, resulting in a differential-algebraic equation (DAE) system. These equations must be satisfied at every time step. Therefore, these equations are used as constraints in the optimization problem. There are also other other limitations to the system that can be described as inequality constraints. These can be limitations to how large the change in the input can be, or how large the input in itself can be. In general, the constraints can be written as [8]:

$$\dot{x} = f(x, z, p, u) \tag{15a}$$
$$0 = g(x, z, p, u) \tag{15b}$$
$$0 \leq h(x, z, p, u) \tag{15c}$$

Where $\dot{x}$ describes the set of differential equations, x are the differential states, z is the set of algebraic states, p are the parameters of the system and u is the input to the system. g is the set of algebraic constraints and h is the set of inequality constraints.

4.1 Solving Differential Algebraic Systems

To solve differential algebraic equation systems, some possible solutions are to use either a sequential or a simultaneous approaches [8]. In sequential approaches such as single shooting, the equations of the models and the optimization problem are solved sequentially to an accepted level of tolerance. On the other hand, simultaneous approaches such as multiple shooting or orthogonal collocation solve the model equations simultaneously with the optimization problem. In general, the simultaneous approaches will have a lower computational cost than the sequential approaches [8]. Orthogonal collocation has been chosen as the preferred way of solving the dynamic algebraic equation system in this thesis for its low computational cost and its accurate results.

Orthogonal collocation on finite elements bases itself on dividing the prediction horizon into finite elements. Each of these elements are again divided into a given amount of collocation points. A usual amount of collocation points is three, and is also what is used for this thesis. The set of differential equations can be written as:

$$M \begin{bmatrix} \dot{x}_1 \\ \dot{x}_2 \\ \dot{x}_3 \end{bmatrix} = \begin{bmatrix} x_1 \\ x_2 \\ x_3 \end{bmatrix} - \begin{bmatrix} x_0 \\ x_0 \\ x_0 \end{bmatrix} \tag{16}$$

Where M is the collocation weighting matrix. The state trajectory can be approximated as:

$$x(t) = A + Bt + Ct^2 + Dt^3 \tag{17}$$

Where t is the placement of the collocation points on the finite element. The derivative of x with respect to t is given by:

$$\dot{x}(t) = B + 2Ct + 3Dt^2 \tag{18}$$

Inserting Eq. (17) and Eq. (18) into Eq. (16) gives:

$$M \begin{bmatrix} B + 2Ct_1 + 3Dt_1^2 \\ B + 2Ct_2 + 3Dt_2^2 \\ B + 2Ct_3 + 3Dt_3^2 \end{bmatrix} = \begin{bmatrix} A + Bt + Ct_1^2 + Dt_1^3 \\ A + Bt + Ct_2^2 + Dt_2^3 \\ A + Bt + Ct_3^2 + Dt_3^3 \end{bmatrix} - \begin{bmatrix} x_0 \\ x_0 \\ x_0 \end{bmatrix} \tag{19}$$

Noticing that if $A = x_0$, then:

$$M \begin{bmatrix} 1 & 2t_1 & 3t_1^2 \\ 1 & 2t_2 & 3t_1^2 \\ 1 & 2t_3 & 3t_1^3 \end{bmatrix} \begin{bmatrix} B \\ C \\ D \end{bmatrix} = \begin{bmatrix} t_1 & t_1^2 & t_1^3 \\ t_1 & t_2^2 & t_2^3 \\ t_1 & t_3^2 & t_3^3 \end{bmatrix} \begin{bmatrix} B \\ C \\ D \end{bmatrix} \tag{20}$$

This yields the following weighting matrix, M:

$$M = \begin{bmatrix} t_1 & t_1^2 & t_1^3 \\ t_1 & t_2^2 & t_2^3 \\ t_1 & t_3^2 & t_3^3 \end{bmatrix} \begin{bmatrix} 1 & 2t_1 & 3t_1^2 \\ 1 & 2t_2 & 3t_1^2 \\ 1 & 2t_3 & 3t_1^3 \end{bmatrix}^{-1} \tag{21}$$

Having the weighting matrix, M, it is possible to solve Eq. (16) for every finite element. The positioning of the collocation points was chosen to be the Gauss-Radau which are given by: $[0.1151, 0.6449, 1.0000]$. By using the Gauss-Radau collocation points there is no need to interpolate at the end of every finite element as the last collocation point in the Gauss-Radau collocation points is 1. For intervals that are not between 0 and 1, a scaling parameter h is introduced.

To solve this system for a DAE system, the algebraic constraints, g, must be evaluated at every collocation point. Substituting Eq. (15a) into Eq. (16) and introducing the scaling parameter, h, gives:

$$\begin{bmatrix} x_1 \\ x_2 \\ x_3 \end{bmatrix} = \begin{bmatrix} x_0 \\ x_0 \\ x_0 \end{bmatrix} + hM \begin{bmatrix} f(x_1, z_1, p_1, u_1) \\ f(x_2, z_2, p_2, u_2) \\ f(x_3, z_3, p_3, u_3) \end{bmatrix} \tag{22}$$

A constraint on the differential states, x, is enforced within every collocation point and at the end of every collocation point to ensure that the trajectory for the differential states are continuous. The objective function is evaluated at the end of every collocation point. The objective function in Eq. (14) with the constraints given in Eq. (15) and by the use of orthogonal collocation, becomes a non-linear optimization program. This problem is solved using the IPOPT solver [9].

5 Data Driven Modellling

Data driven models are obtained based on previously recorded data to calculate the weights for the system. These weights are used together with the history of the current system to calculate a new prediction of the output. The models that will be discussed in this thesis are auto-regressive exogenous input (ARX), auto-regressive moving average exogenous input (ARMAX) and output error (OE) model.

5.1 ARX Model

The ARX model is based on previous measurements of inputs and also outputs. Such structure can be described by [10]:

$$A(q)y(t) = B(q)u(t) + e(t) \tag{23}$$

Where q is the shift operator which is used to denote previous or future values. $u(t)$ describes the inputs and $e(t)$ describes the errors at time t.

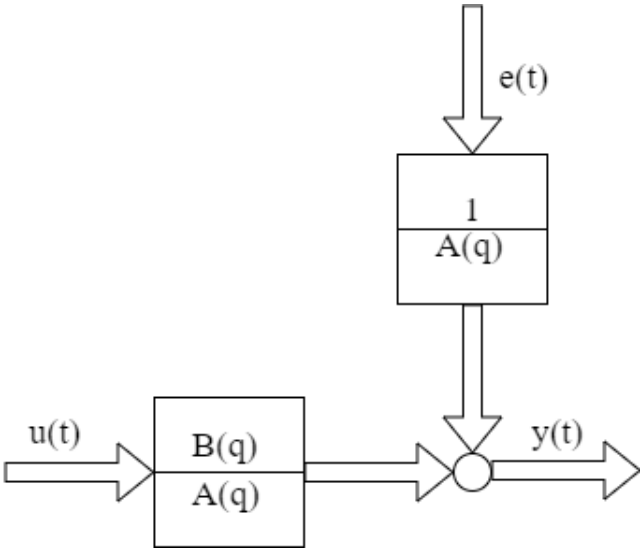

Figure 5: The ARX model structure [10].

The structure for the ARX model can also be described by the block diagram shown in Fig. 5. $A(q)$ and $B(q)$ are a function of the shift operator and given by:

$$A(q) = \sum_{k=0}^{n_a} a_k q^{-k} = a_0 + a_1 q^{-1} + ... + a_{n_a} q^{-n_a} \tag{24}$$

$$B(q) = \sum_{k=1}^{n_b} b_k q^{-k} = b_1 q^{-1} + b_2 q^{-2} + ... + b_{n_b} q^{-n_b} \tag{25}$$

Where $a_0 = 1$. n_b and n_a are tuning parameters that describe how many previous values of the outputs, $y(t)$, and the inputs, $u(t)$, respectively that will be used when creating the model. n_k is a parameter which describes the dead time, leading to $b_1, ..., b_{n_k} = 0$. It is possible to write the ARX model as a linear model:

$$\hat{y}(t, \nu) = \phi(t)^T \nu \tag{26}$$

Where $\hat{y}(t, \nu)$ describes the predicted output for a given point in time. $\phi(t)$ describes the previous outputs and inputs, giving $\phi(t) = [-y(t-1), -y(t-2), ..., -y(t-n_a), u(t-1), u(t-2), ..., u(t-n_b)]^T$. ν describes all the weights of the previous outputs and inputs: $\nu = [a_1, a_2, ..., a_{n_a}, b_1, b_2, ..., b_{n_b}]^T$. Given the total number of observations, $N >> \max(n_a, n_b)$, it is possible to make a regressor matrix or design matrix. Given $n_a \geq n_b$, the regressor matrix is given by:

$$\Phi = \begin{bmatrix} -y(n_a-1) & \cdots & -y(0) & u(n_a-1) & \cdots & u(n_a-n_b) \\ -y(n_a) & & -y(1) & u(n_a) & \cdots & u(n_a-n_b+1) \\ -y(n_a+1) & & \vdots & & \vdots & \\ \vdots & & & & & \\ -y(N-1) & \cdots & -y(N-n_a) & u(N-1) & \cdots & u(N-n_b) \end{bmatrix} \tag{27}$$

Thus, it is possible to find the weights, ν, by using an ordinary least squares estimator which gives the following solution:

$$\hat{\nu} = (\Phi^T \Phi)^{-1} \Phi^T y \tag{28}$$

The procedure for finding the least squares estimator is given in Appendix D.

5.2 ARMAX Model

The ARMAX model is based on previous measurements of the input and output, but also on the errors from previous measurements. The model structure can be written as [10]:

$$A(q)y(t) = B(q)u(t) + C(q)e(t) \tag{29}$$

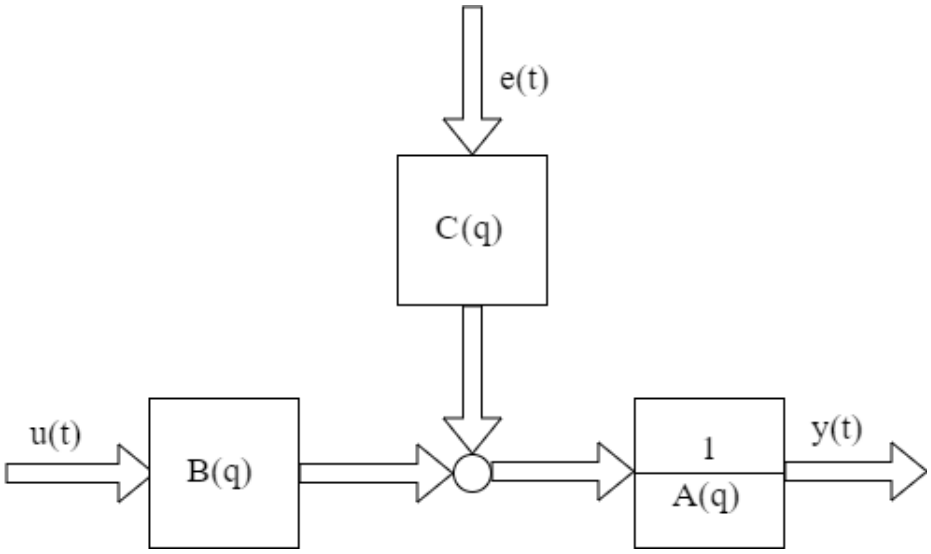

Figure 6: Structure of the ARMAX model [10].

As for the ARX model, a block diagram can also show the structure of the ARMAX model which is given in Fig. 6. $C(q)$ is a function of the shift operator, q, and is given by:

$$C(q) = \sum_{k=0}^{n_c} c_k q^{-k} = c_0 + c_1 q^{-1} + c_2 q^{-2} + \ldots + c_{n_c} q^{-n_c} \tag{30}$$

Where $c_0 = 1$ and n_c describes how many previous values of the errors, $\varepsilon(t)$, that will be used when creating the model. Similarly to the ARX model, it is possible to write the ARMAX model as a linear model.

$$\hat{y}(t,\nu) = \phi(t,\nu)^T \nu \tag{31}$$

Where $\nu = [a_1, a_2, ..., a_{n_a}, b_1, b_2, ..., b_{n_b}, c_1, c_2, ..., c_{n_c}]^T$ also includes the weights for the errors and $\phi(t,\nu) = [-y(t-1), -y(t-2), .. - y(t-n_a), u(t-1), u(t-2), ..., u(t-n_b), \varepsilon(t-1,\nu), e(t-2,\nu), ..., \varepsilon(t-n_c,\nu)]^T$. Although, the error terms, ε, are unknown. Usually these errors are substituted by prediction errors, namely:

$$\varepsilon(t,\nu) = y(t,\nu) - \hat{y}(t,\nu) \tag{32}$$

The regressor matrix for $n_a \geq n_b, n_c$ then becomes:

$$\Phi^{(i)} = \begin{bmatrix} y(n_a-1) & \cdots & y(0) & u(n_a-1) & \cdots & u(n_a-n_b) & \varepsilon(n_a-1,\hat{\nu}^{i-1}) & \cdots & \varepsilon(n_a-n_c,\hat{\nu}^{(i-1)}) \\ y(n_a) & & y(1) & u(n_a) & \cdots & u(n_a-n_b+1) & \varepsilon(n_a,\hat{\nu}^{(i-1)}) & & \varepsilon(n_a-n_c,\hat{\nu}^{(i-1)} \\ y(n_a+1) & & \vdots & \vdots & & \vdots & \vdots & & \vdots \\ \vdots & & & & & & & & \\ y(N-1) & \cdots & y(N-n_a) & u(N-1) & \cdots & u(N-n_b) & \varepsilon(N-1,\hat{\nu}^{(i-1)}) & \cdots & \varepsilon(N-n_c,\hat{\nu}^{(i-1)}) \end{bmatrix} \tag{33}$$

Since the error term is a function of the weights, ν, it is not possible to calculate the weights directly and an iterative method is thus needed. For the first iteration, $i = 0$, a least squares solution is usually used. This gives the same regressor matrix as for the ARX model as shown in Eq. (27) and $\nu^{(0)}$ is calculated by Eq. (28). For further iterations an extended least squares method is used [10]. In this iteration scheme, the previous iteration gives the prediction error which can be used for the next iteration. This algorithm is repeated until convergence or until the algorithm reaches its maximum number of iterations. The following algorithm can be used for finding the weights [10]:

Algorithm 1: Algorithm for calculating the weights of an ARMAX model.

Choose the parameters n_a,n_b and n_c;
Given $n_a \geq n_b, n_c$, define the regressor matrix, $\Phi^{(0)}$, as shown in Eq. (27);
Find the weights, $\nu^{(0)}$, by finding the least squares estimator as described in Eq. (28);
Calculate the error terms, as: $\varepsilon = y - \hat{y}(t,\nu^{(0)})$;
for *i= 1:K* **do**
    Find the regressor matrix, $\Phi^{(i)}$ shown in Eq. (33);
    Calculate the weights, $\nu^{(i)}$, by the least squares estimator given by Eq. (28);
    Update the error terms: $\varepsilon = y - \hat{y}(t,\nu^{(i-1)})$;
    if *convergence* **then**
        break;
    end
end

The for-loop will repeat until a chosen maximum number of iterations, K, or until convergence [10].

5.3 OE Model

In the output error (OE) model, it is assumed that the only noise of the model is white measurement noise. Thus the model can be defined as [10]:

$$\xi(t) + f_1\xi(t-1) + ... + f_{n_f}\xi(t-n_f) = b_1u(t-1) + b_2u(t-2) + ... + b_{n_b}u(t-n_b) \quad (34)$$

Where $\xi(t) = y(t) - e(t)$ describes the output of the system without noise and $f_1, ..., f_{n_f}$ is the weightings for the noise free outputs. This can be rewritten as:

$$y(t) = \frac{B(q)}{F(q)}u(t) + e(t) = \xi(t) + e(t) \quad (35)$$

B(q) is as described in Section 5.2 and F(q) is:

$$F(q) = \sum_{k=0}^{n_f} f_k q^{-k} = 1 + f_1q^{-1} + f_2q^{-2} + ... + f_{n_f}q^{-n_f} \quad (36)$$

Where n_f is a tuning parameter. The model structure of the OE model as given in Eq. (35) can also be written as a block diagram which is shown in Fig. 7.

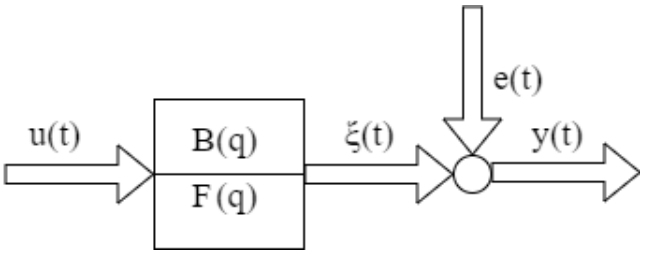

Figure 7: Structure of the OE model [10].

As seen in Section 5.1 and Section 5.2, this model structure can also be rewritten as a linear model:

$$\hat{y}(t, \nu) = \phi(t, \nu)^T \nu \quad (37)$$

Where $\phi(t, \nu)$ consisting of the inputs and the noise free outputs: $\phi(t, \nu) = [u(t-1), u(t-2), ..., u(t-n_b), \xi(t-1, \nu), \xi(t-2, \nu), \xi(t-n_f, \nu)]^T$ and $\nu = [b_1, b_2, ..., b_{n_b}, f_1, f_2, ..., f_{n_f}]^T$ is a vector consisting of the weights of the model.

To find the weights, ν, for an OE model, Eq. (35) is first rearranged with setting the noise term to be $v(t) = F(q)e(t)$ which gives:

$$F(q)y(t) = B(q)u(t) + F(q)e(t) = B(q)u(t) + v(t) \quad (38)$$

Although the errors, $e(t)$, may not be correlated, the noise term $v(t)$ will still usually be auto-correlated. This is because $v(t)$ is a moving average since the $F(q)$ term describes previous values [10]. Due to this fact, there is a correlation between Φ and v giving biased estimates of the least squares estimator. By setting $\hat{y}(t,\nu) = \xi(t,\nu)$, the correlation can be avoided, but this will need an instrumental variable method which is an iterative method to be solved [10]. With $n_f \geq n_b$, the instrumental variable is given by:

$$Z^{(i)} = \begin{bmatrix} \xi(n_f - 1, \hat{\nu}^{(i-1)}) & \cdots & \xi(0, \hat{\nu}^{(i-1)}) & u(n_f - 1) & \cdots & u(n_f - n_b) \\ \xi(n_f, \hat{\nu}^{(i-1)}) & & \xi(1, \hat{\nu}^{(i-1)}) & u(n_f) & \cdots & u(n_f - n_b + 1) \\ \xi(n_f + 1, \hat{\nu}^{(i-1)}) & & \vdots & \vdots & & \vdots \\ \vdots & & \vdots & \vdots & & \vdots \\ \xi(N-1, \hat{\nu}^{(i-1)}) & \cdots & \xi(N - n_f, \hat{\nu}^{(i-1)}) & u(N-1) & \cdots & u(N - n_b) \end{bmatrix} \tag{39}$$

Using the least squares estimator, the following result is obtained for the weights of the instrumental variable:

$$\hat{\nu}_{IV} = (Z^T Z)^{-1} Z^T y \tag{40}$$

The constant regressor matrix for $n_f \geq n_b$ is given by:

$$\Phi = \begin{bmatrix} y(n_f - 1) & \cdots & y(0) & u(n_f - 1) & \cdots & u(n_f - n_b) \\ y(n_f) & & y(1) & u(n_f) & \cdots & u(n_f - n_b + 1) \\ y(n_f + 1) & & \vdots & \vdots & & \vdots \\ \vdots & & & & & \\ y(N-1) & \cdots & y(N - n_f) & u(N-1) & \cdots & u(N - n_b) \end{bmatrix} \tag{41}$$

As for the ARMAX model, there is need for an iterative method to solve for the weights. The first iteration of $Z^{(0)}$ is usually done by using least squares method, giving $Z^{(0)} = \Phi$ and the least squares estimator shown in Eq. (28).

The weights for the OE model can be calculated by the following algorithm:

Algorithm 2: Algorithm for calculating the weights of an OE model.

Choose the parameters n_b and n_f;
Define the regressor matrix, Φ, as shown in Eq. (41);
Calculate the weights, $\nu^{(0)}$, from the least squares estimator given that $Z^{(0)} = \Phi$;
Calculate the instrumental variables, $\xi(t, \nu^{(0)})$;
for *i=1:K* **do**
    Define $Z^{(i)}$, as shown in Eq. (39);
    Calculate $\nu^{(i)}$ from Eq. (40);
    Update the instrumental variables, $\xi(t, \nu^{(i)})$;
    if *convergence* **then**
        break;
    end
end

The for-loop will repeat until a chosen maximum number of iterations, K, or until convergence [10].

5.4 Model Selection

With a lot of tuning parameters, there is also a need fot a criterion to decide upon which model is the preferred model. There are several criteria that could be used for this. Although a measurement of prediction error can give an indication whether the model is good or not, there is also a need to assess the complexity of the model as having a less complex model is preferred. Thus there is a trade-off between the least complex model and a model that gives the lowest prediction error.

5.4.1 Normalized Root Mean Square Error

The normalized root mean square error (NRMSE) is a measurement of how well the model fits the test data. Since it is a normalized root, it will also give back a number between $-\infty$ and 1. The value 1 means that the model fits the test data perfectly and a NRMSE trending to $-\infty$ means that the fit is bad. The NRMSE is closely related to the mean square error (MSE), although the MSE is an arbitrary, positive value. The MSE is given by:

$$MSE = \frac{1}{n}\sum_{i=1}^{n}(y_i - \hat{f}(x_i))^2 \tag{42}$$

Where n is the number of observations, y_i is the true response from the training set for the ith observation and $\hat{f}(x_i)$ is the predicted response for the ith observation [11]. The mean of the predicted response is given by $\bar{\hat{f}} = \frac{1}{n}\sum_{i=1}^{n}\hat{f}(x_i)$. This gives the following NRMSE:

$$NRMSE = 1 - \frac{\sqrt{\sum_{i=1}^{n}(y_i - \hat{f}(x_i))^2}}{\sqrt{\sum_{i=1}^{n}(\hat{f}(x_i) - \bar{\hat{f}})^2}} \tag{43}$$

5.4.2 AIC and FPE

The Akaike information criterion (AIC) is based on a trade-off between the fit and the complexity of the model and is given by:

$$AIC = 2n_p - 2L(\nu) \tag{44}$$

Where $L(\nu)$ is the maximum log-likelihood function of the model [12]. n_p describes how many parameters that have been estimated. The AIC states that the best model is the model with the lowest value of AIC.

When the observations are subject to normally distributed errors with constant variance, the maximum log-likelihood function is given by [13]:

$$L(\nu) = -\frac{N}{2}(1 + \ln(2\pi) + \ln(\frac{1}{N}\sum_{t=1}^{N}\varepsilon_t^2)) \tag{45}$$

Where ε are the errors and N is the total number of observations.

Substituting Eq. (45) into Eq. (44) gives:

$$AIC = N + N\ln(2\pi) + N\ln(\frac{1}{N}\sum_{t=1}^{N}\varepsilon_t^2) + 2n_p \tag{46}$$

Another criteria that is used for model selection is the final prediction error (FPE) which is given by:

$$FPE = (\frac{1}{2\cdot N}\sum_{t=1}^{N}\varepsilon_t^2)\cdot\left(\frac{1+\frac{n_p}{N}}{1-\frac{n_p}{N}}\right) \tag{47}$$

The FPE describes the variance of the prediction error that is expected when testing the model with a different data set than the one used for training the model [13]. Thus, a lower FPE will also yield a better model.

6 Results and Discussion

The results will be divided into two separated parts. The first part will be focusing on making a model predictive controller to control erosion of the chokes in the gas lifted well system. The goal of this part is to maximize the total production of oil while keeping the erosion of each production

choke below a set threshold. The second part will be focused on making data driven models from simulated data. The goal is to identify whether it is possible to use data driven models to model erosion and to find the best suited model for this purpose. This thesis will not be looking into combining the two parts, but this is suggested as a task for future work. It should be noted that these results are based on an ideal case as the simulated data is used to make the data driven models in addition to the model for the non linear problem in the MPC.

All of the system simulations were done in MATLAB. The script for simulating the system is based on the equations of the gas lifted well network as given in Section 3.1 and the erosion model given in Section 3.2. For integrating the system and for optimization purposes, CasADi was used [14]. CasADi provides useful tools for nonlinear optimization and is an open-source software. The IPOPT solver was used to solve the non linear programming problems. All the used scripts in this thesis can be found on Github: `https://github.com/JoachimAgotnes/project_thesis`.

Due to the large time scale difference between the erosion rate and the differential equations in the gas lift model, Eq. (1), the differential equations in the gas lift model were set to be algebraic equations, meaning that the equations in Eq. (1) can be rewritten as:

$$0 = w_{gl} - w_{iv} \tag{48a}$$
$$0 = w_{iv} - w_{pg} + w_{rg} \tag{48b}$$
$$0 = w_{ro} - w_{po} \tag{48c}$$

This assumption is used throughout the thesis.

6.1 Controlling Erosion in a Gas Lifted Well Network

A model predictive controller for the erosion model in the gas lifted well system was made with the goal of maximizing the total production of oil while satisfying a constraint on the maximum allowed erosion for each well. The constraint on the erosion, E_{max}, is set to a maximum of 2.1 mm for each well.

The differential equation given in Eq. (13) and the algebraic equations given in Section 3.2 and Section 3.1 are also constraints for the MPC problem. The optimization problem for the controller

can be written as:

$$\min \int_0^{t_p} \left(\sum_{i=1}^{3} -w(t)_{i,po} + \frac{1}{2}\Delta u(t)^T R_{\Delta u} \Delta u(t) + \sum_{i=1}^{3} \rho_{i,s} s_i(t) \right) dt \tag{49a}$$

s.t.

$$\frac{dE}{dt} = \frac{K \cdot F(\alpha) \cdot U_p^n}{\rho_t \cdot A_t} \cdot G \cdot C_1 \cdot GF \cdot \dot{m}_p \cdot C_{unit} \qquad t \in [0, t_p] \tag{49b}$$

$$g(x) = 0 \qquad t \in [0, t_p] \tag{49c}$$

$$\Delta u(t) = 0 \qquad t \in [t_m, t_p] \tag{49d}$$

$$-\Delta u_{max} \leq \Delta u(t) \leq \Delta u_{max} \qquad t \in [0, t_m] \tag{49e}$$

$$u_{min} \leq u(t) \leq u_{max} \qquad t \in [0, t_p] \tag{49f}$$

$$0 \leq E(t) + s(t) \leq E_{max} \qquad t \in [0, t_p] \tag{49g}$$

Where $g(x)$ describes the algebraic model equations in Section 3.1 and Section 3.2. The last term in Eq. (49a), $s_i(t)$, describes a slack term that was added to the objective function given in Eq. (14). This slack term was also added to the constraint on the erosion. This gives the controller the opportunity to violate the constraint, but at a high cost for the objective function as the weighting parameters, as $\rho_{1,s} = \rho_{2,s} = \rho_{3,s} = 99999$. As the change in the gas lift rate only changes the slope of the erosion for each well, there will be erosion even at the lowest value of the gas lift rate. When the controller realizes it may violate the erosion bounds it will try to change the gas lift rate during the prediction horizon in a way that does not violate this condition. However, it may be impossible and thus it may enter an infeasible region where the controller can not satisfy the constraint on the maximum erosion. The slack variable ensures that this region will still give feasible solutions. t_m describes the input horizon, while t_p is the prediction horizon and $\Delta u(t) = u(t) - u(t-1)$.

The regularization term on Δu will not have a great impact on the stability of the controller as the controller is stable by itself. Although the term is not removed in case of further modifications to the system. The weighting on the regularization, $R_{\Delta u}$, was set to be:

$$R_{\Delta u} = \begin{bmatrix} 1 & 0 & 0 \\ 0 & 1 & 0 \\ 0 & 0 & 1 \end{bmatrix} \tag{50}$$

The method used for solving the differential algebraic equation was orthogonal collocation. The algebraic equations were implemented as constraints at every collocation point. To ensure flow, a minimum input of $0.4\mathrm{kg\,s^{-1}}$ for the gas lift mass rate was chosen while the upper limit was set to $u_{max} = 2\mathrm{kg\,s^{-1}}$. A conservative value of $\Delta u_{max} = 0.01\mathrm{kg\,s^{-1}}$ was chosen. As each time step is a day, computational issues are low, and therefore a long prediction horizon of 100 days was chosen as well as an input horizon of 70 days. Since a change in input only changes the slope of the erosion, a long prediction horizon is needed for the controller to be able to meet the constraint on the erosion threshold. After simulating the MPC for 500 days, the following result was obtained:

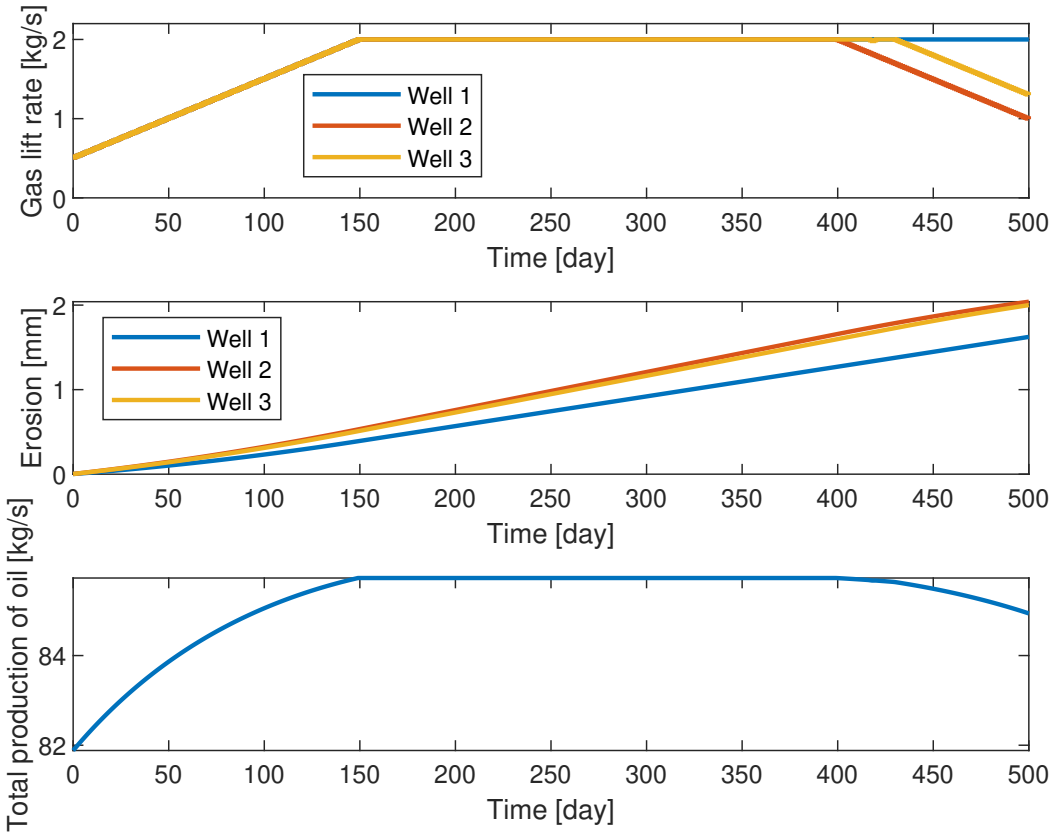

Figure 8: MPC with a threshold value of erosion of below 2.1 mm.

From the simulation results as shown in Fig. 8, the controller maximizes the total production of oil by increasing the gas lift rate as fast as possible only being held back by the limit of Δu_{max}. When the gas lift rate is constant at its max limit, the slope of the erosion and the total production of oil is also constant. When the controller realizes it will violate the constraint on the erosion threshold it will start decreasing the gas lift rate. As seen in Fig. 9, the second well has the highest extent of erosion when applying the same input to all the wells. Due to the lower *GOR* and reservoir pressure, well 1 will be the least exposed to erosion given the same gas lift rate. This is also why the gas lift rate is decreased in well 2 first and then well 3. There is no decrease in the gas lift rate for well 1 as it is not near the threshold. The total production of oil is the highest when the gas lift rate is at the maximum for all the wells. It decreases when the gas lift rate of well 2 and 3 decreases towards the end of the simulation. The controller does not violate the constraint on erosion and is thus successful in keeping the erosion in each well below the set threshold.

It should be noted that there is an error in the simulated response in Fig. 8, as well 3 has a small decrease in the gas lift rate at around day 400. The gas lift rate in well 3 seems to be dependent on the gas lift rate in well 2. Due to time limitations of this project, the reasoning behind this error could not be found, but it should be looked into further.

6.2 Modelling Erosion with the use of Data Driven Modelling

First a data set was made from simulations of erosion of a choke in a gas lifted well network. The data set was divided into a training data set and a test data set. The training data was used to train all the models, while the test set was used to test the model on. When creating a model, it is important to test on different data to guarantee that the model is not overfitting the training data. If this model was to be tested on the same set as it was trained on, it is very likely that it would overestimate the prediction capabilities of the model. The training and test set were made in the same way, although the changes in input were different. For simplicity, only the training set is described in the following section.

6.2.1 Simulation Data

The parameters for each well can be found in Table 8 and the riser parameters can be found in Table 7. The system was modelled with three wells and one riser system. The gas lift rate, w_{gl}, for each well as the input for the system and the erosion for each choke in each well, E, as the output measurement. The system was simulated for 500 periods, with each period being 1 day. For the purpose of identification, two changes to the input were made. The inputs for the training set is igven in Table 1 and the inputs for the test set is given in Table 2.

Table 1: Gas lift rate, w_{gl}, for the training set.

Period	Value
1-150	$0.35\,\mathrm{kg\,s^{-1}}$
151-200	$0.50\,\mathrm{kg\,s^{-1}}$
201-300	$0.85\,\mathrm{kg\,s^{-1}}$

Table 2: Gas lift rate, w_{gl}, for the test set.

Period	Value
1-200	$0.50\,\mathrm{kg\,s^{-1}}$
201-350	$0.75\,\mathrm{kg\,s^{-1}}$
351-500	$0.25\,\mathrm{kg\,s^{-1}}$

It is assumed that the degradation of the chokes in the wells do not affect the flow through the system and that the sand rate, $\dot{m}_p$, is constant. Measurement noise was added to the system as Gaussian distributed noise with a mean of 0 mm and a standard deviation of 0.01 mm. This value is although believed to be conservative as a measurement of the erosion with a standard deviation of 0.01mm may be difficult to obtain.

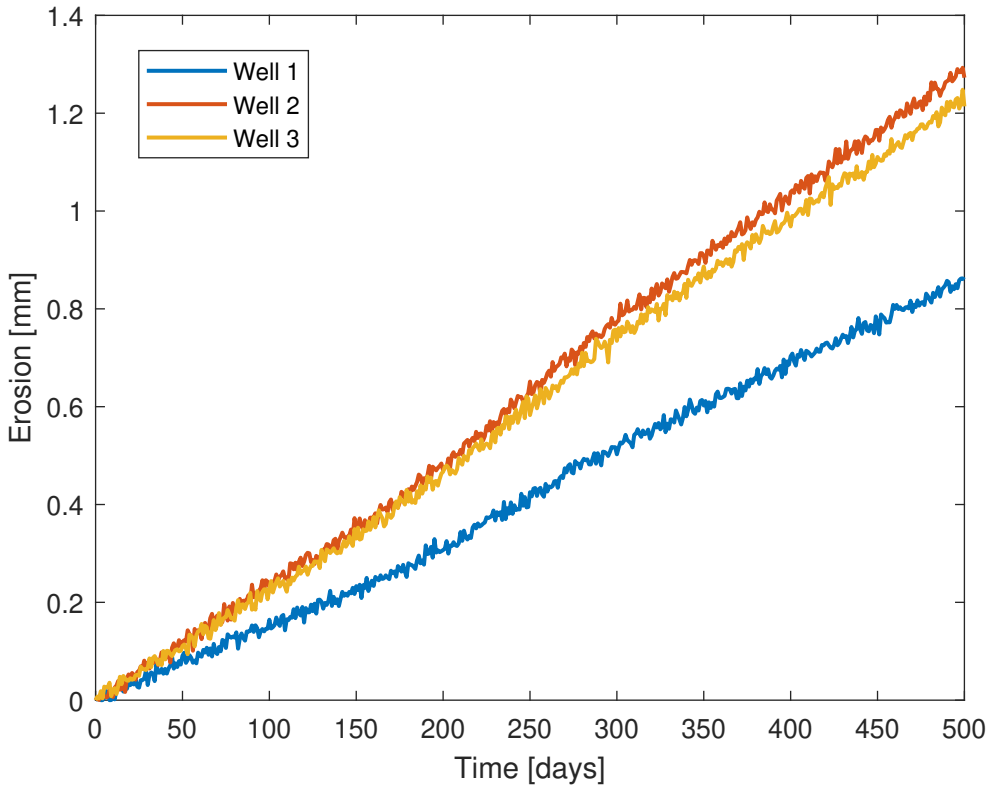

Figure 9: Results from simulating erosion with a step change with 3 wells.

As seen from Fig. 9, the erosion rate in each well is almost linear. The change in the gas lift rate, w_{gl}, changes the slope for all of the wells which can be seen at day 151 and at day 201. An increase in the gas lift rate, w_{gl} will also increase the pressure in the annulus, increasing the mass flow rate through both the injection valve and the production valve. A higher mass flow rate through the production valve of both oil and gas will give an increase in the characteristic impact velocity of the sand particles onto the valve, causing a higher grade of erosion. The extent of erosion in the second and third well is much higher than in the first well. Most of the well specific parameters in Table 8 are the same except the reservoir pressure and the *GOR*.

Having a lower reservoir pressure will decrease the mass flow rate of both oil and gas from the reservoir, thus decreasing the produced oil and gas which again leads to a lower grade of erosion. Having a lower GOR will decrease the ratio of gas and oil. Utilizing that $GOR = \frac{Q_{pg}}{Q_{po}}$ and putting it into Eq. (53) gives:

$$Q_m = Q_{po} + Q_{pg} = (1 + GOR) \cdot Q_{po} \tag{51}$$

Decreasing the *GOR* will therefore also decrease the mixed volumetric flow, Q_m. Consequently, also the impact velocity of the sand particles decrease, giving less erosion. A lower *GOR* means that the flow will be more dense and have a higher viscosity. For flows with higher density, the sand particles tend to be carried with the streamlines of the flow, rather than in a straight line as

for lower density flows [4]. This means that the impact velocity will be lower than for flows with higher *GOR*, which are flows that have a higher gas content, meaning a lower density.

Well 1 in Fig. 9 has the lowest erosion over the time horizon which makes sense since it has lower *GOR* and reservoir pressure than the two other wells. Well 2 and well 3 have similar extent of erosion, but due to the higher *GOR*, the choke of well 2 will erode fast than the choke of well 3.

6.2.2 Data Driven Modelling

Assuming that the flows in the wells different wells do not interact with each other, data driven models were created for each individual well. All the parameters were varied from 1 to 20, without the dead time, n_k which was varied from 0 to 1. All the models within this segment were created and tested against the test set, giving a value for the NRMSE.

In order to compare the models, model selection was needed to find the preferred or best model for each well. The AIC and FPE were used to determine which model was the best for each type of data driven model for each well.

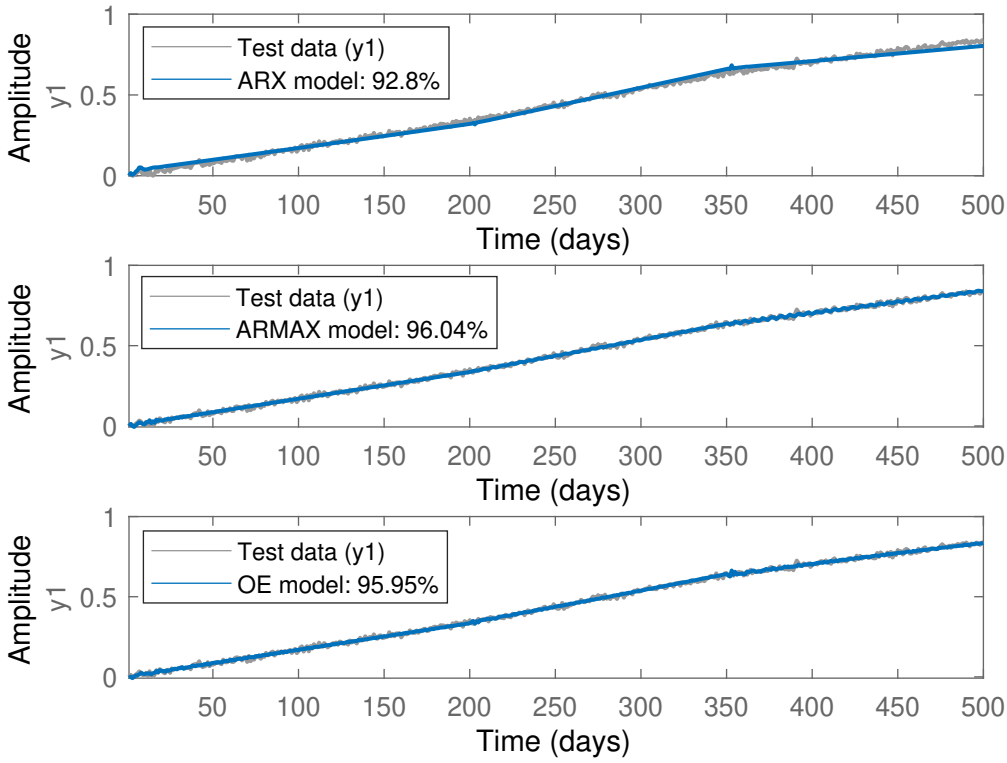

Figure 10: Best ARX, ARMAX and OE models for well 1 plotted against the test set. y_1 is the erosion in mm.

Table 3: Data driven models with lowest AIC and FPE for well 1.

Model type	Model selection criteria	NRMSE	n_a	n_b	n_c	n_f	n_k
ARX	AIC & FPE	92.80%	9	3	-	-	1
ARMAX	AIC & FPE	96.04%	12	2	9	-	1
OE	AIC & FPE	95.95%	-	17	-	16	0

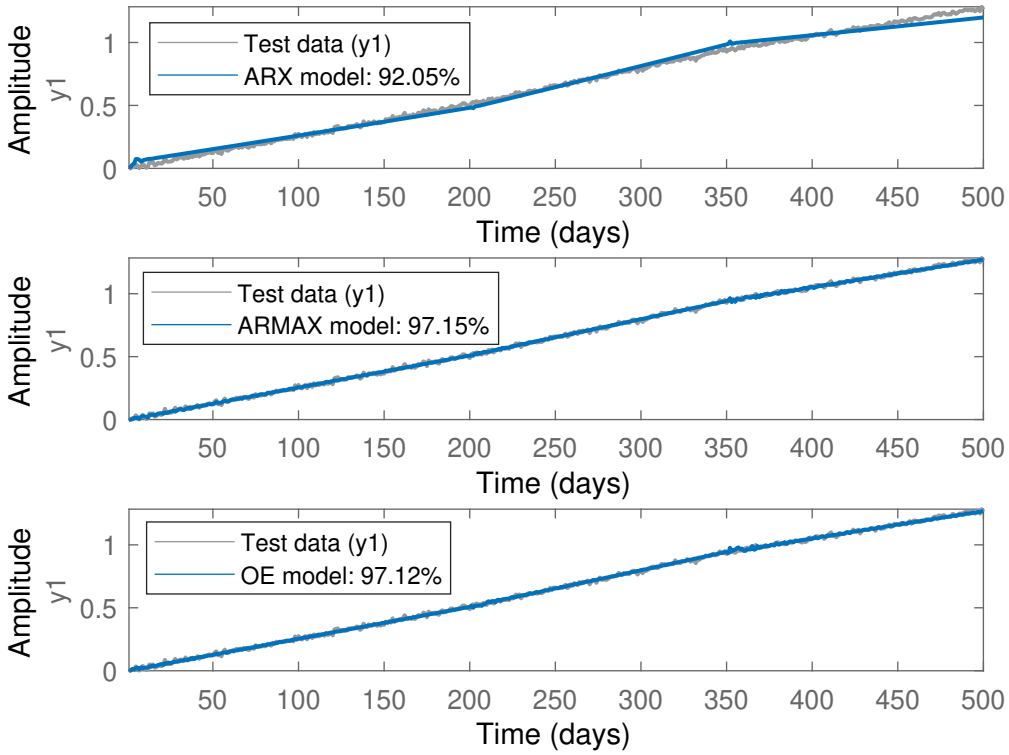

Figure 11: Best ARX, ARMAX and OE models for well 2 plotted against the test set. y_1 is the erosion in mm

Table 4: Data driven models with lowest AIC and FPE for well 2.

Model type	Model selection criteria	NRMSE	n_a	n_b	n_c	n_f	n_k
ARX	AIC & FPE	92.05%	7	2	-	-	1
ARMAX	AIC & FPE	97.15%	15	3	13	-	1
OE	AIC & FPE	97.12%	-	17	-	18	0

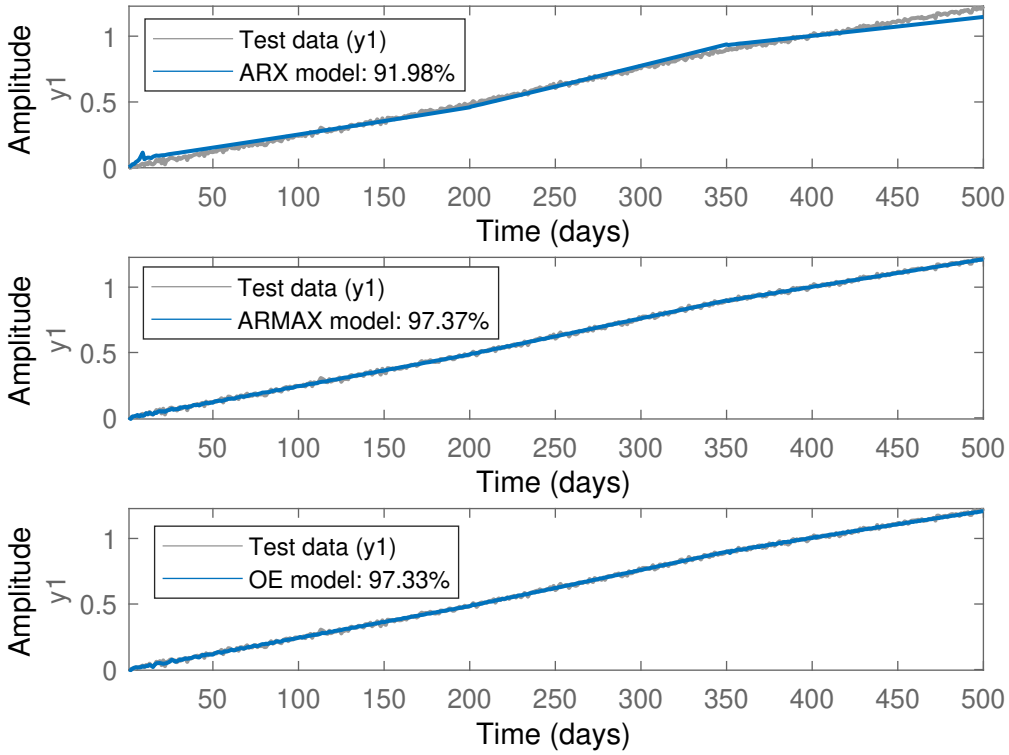

Figure 12: Best ARX, ARMAX and OE models for well 3 plotted against the test set. y_1 is the erosion in mm

Table 5: Data driven models with lowest AIC and FPE for well 3.

Model type	Model selection criteria	NRMSE	n_a	n_b	n_c	n_f	n_k
ARX	AIC & FPE	91.98%	9	1	-	-	0
ARMAX	AIC	97.30%	18	6	20	-	1
ARMAX	FPE	97.37%	10	2	10	-	0
OE	AIC & FPE	97.33%	-	2	-	19	1

In general for all three wells, the ARX is outperformed by both the OE and the ARMAX models. From looking at the ARX models in Fig. 10, Fig. 11 and Fig. 12, it is possible to see that the model changes the slope of the erosion in all wells, but fails to do this accurately, thus making the NRMSE lower. In the plots for the ARMAX and OE models for each well, the models fit the test data very well.

From comparing Table 3, Table 4 and Table 5 the ARMAX and OE models for each well, it is obvious that they have a very similar NRMSE. For the ARMAX model in well 3, the AIC and FPE do not coincide upon which model is the preferred model. Although both the models are have approximately the same NRMSE, the model which the FPE favors is a simpler model with lower

values for the parameters, meaning that the model requires less history of the system and fewer weights have to be calculated. For all these wells, both the ARMAX model and the OE model could be used with great success. Although there is also a need to check the residual plots to see if the residuals are autocorrelated with each other or if the residuals are correlated with the inputs. Although similar plots are made for all of the ARMAX and OE models, only the residual plots for well 1 will be shown as the plots for the other models in the other wells show no significant autocorrelation between the residuals or a correlation between the input and the residuals. Since the ARMAX and OE outperforms the ARX model, the ARX model will not be considered further.

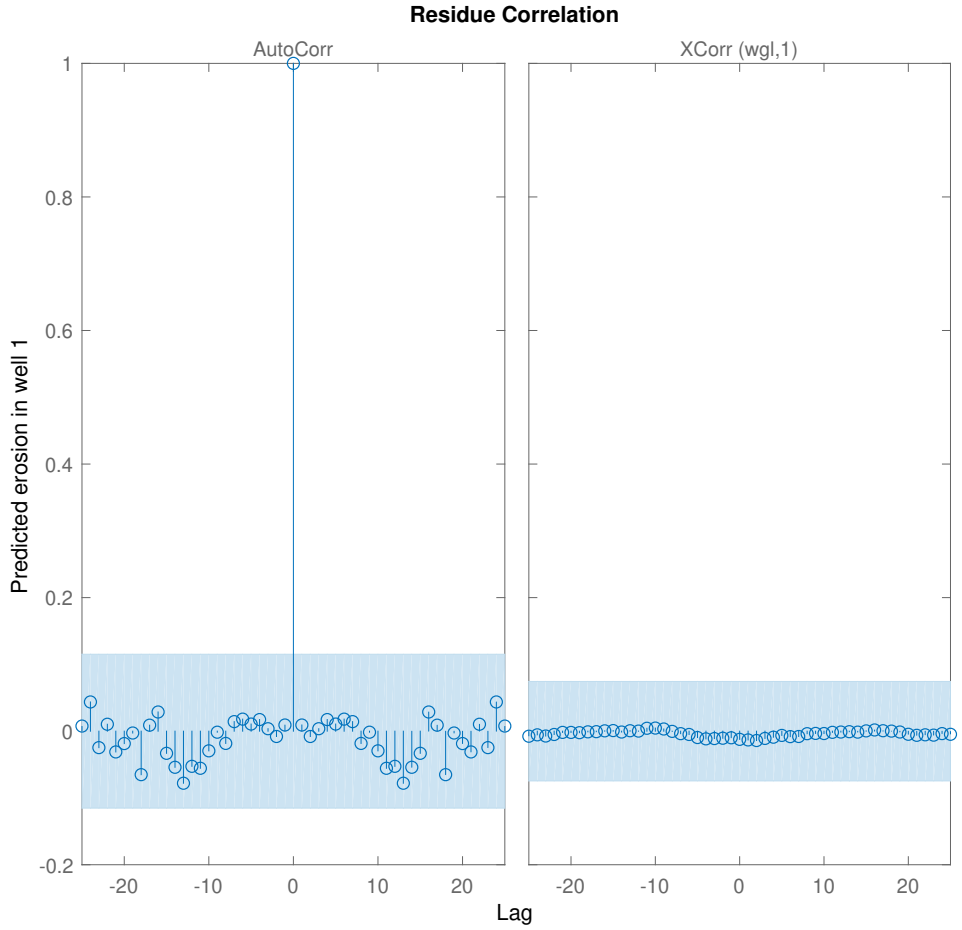

Figure 13: Residual plot for the ARMAX model for well 1.

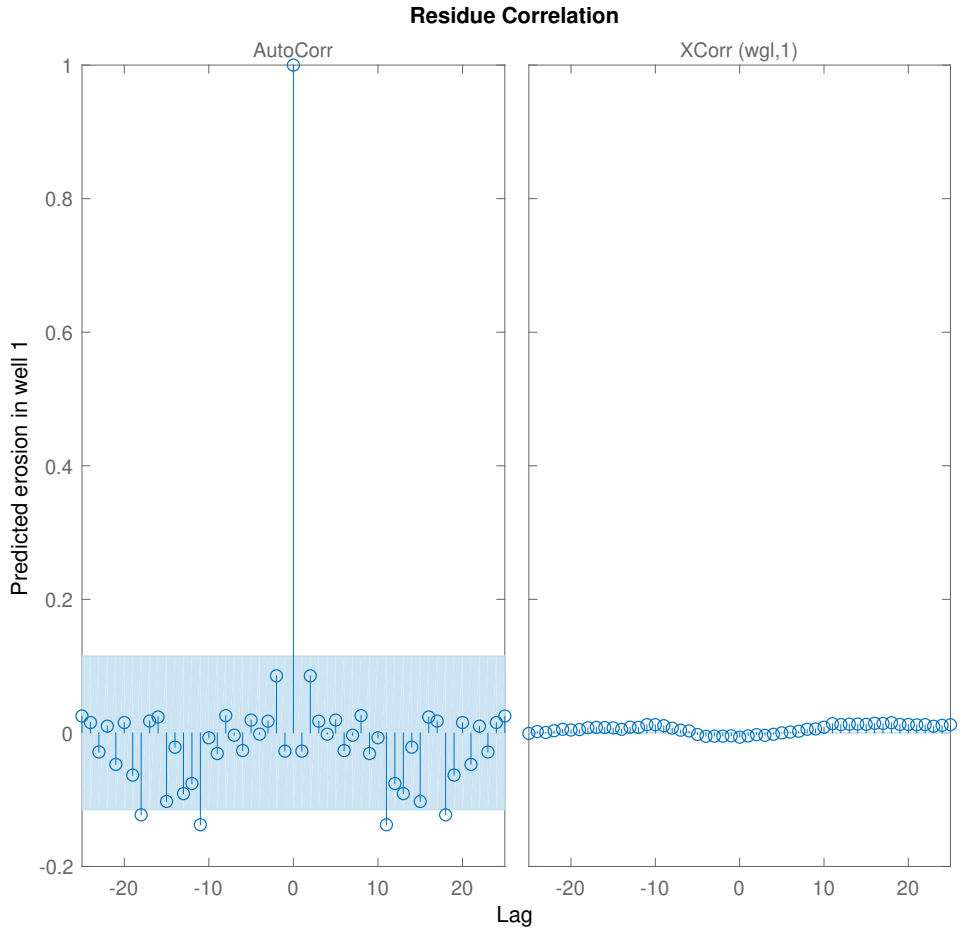

Figure 14: Residual plot for the OE model for well 1

The residual plots in Fig. 13 and Fig. 14 show the autocorrelation of the residuals as well as the correlation between the inputs and the residuals for lag between -25 and 25. The lag describes how many steps ahead in time and how many steps back in time the correlations are looked at. The grey area describes a 99% confidence region. As seen in the residual plot for the ARMAX model given in Fig. 13, there is only a significant autocorrelation term when the lag is 0, at which point all the residuals will be autocorrelated with itself. There are no significant correlations between the inputs and the residuals.

For the residual plot for the OE model given in Fig. 14, there are some autocorrelated residuals that are significant. Also all of the inputs are significantly correlated with the residuals. Although, the model was created on data with a known noise component. The noise added to the system had a constant variance and a mean of 0 mm. This should mean that there should be no correlation between the residuals and the inputs. Why Fig. 14 shows a significant correlation is not known and should be looked for further work, but a safe choice is to use the ARMAX model instead of the OE model for well 1. For well 2 the ARMAX model is chosen as it has a better NRMSE than the other models. For well 3 the ARMAX model chosen based on FPE is the preferred model as it had

a higher NRMSE.

7 Conclusion

An economic MPC controller was made with the goal of maximizing the total oil production with regularization terms and slack variables while keeping the erosion under a certain threshold. The controller was implemented in MATLAB. The results show that a long prediction horizon is needed for the controller to be able to adjust the gas lift rate in order to keep below the set threshold as the change in gas lift rate only changes the slope of the erosion. The controller is successful in keeping the erosion of all of the wells below the threshold, although more work is needed to make the MPC work better.

An erosion model for a choke in a gas lifted well system was created for three separate wells combined in a riser system. Due to a time scale difference, all the differential equations of the gas lifted well system was set as algebraic equations while keeping the erosion rate as a differential algebraic equation. Simulations were done using CasADi in MATLAB with simulations lasting for 500 days with sampling time of 1 day. The slope of the erosion was deemed to be almost constant. When increasing the gas lift rate the slope of the erosion also increased.

Lastly, data driven models were made as an alternative to the phenomenological erosion model. Model selection was done using AIC and FPE. The ARX model was greatly outperformed by the ARMAX and OE model, which both performed approximately equally, obtaining an NRMSE of 96% on well 1 and 97% on well 2 and 3. The ARMAX model was preferred for well 1 as the OE model had autocorrelated residuals and significant correlations between the input and the residuals. For the other wells, both the ARMAX and OE models had no significant trends in the residual plots.

There is a lot of further work that should be done on this topic. This thesis covers modelling of erosion and the use of a model predictive controller to control the erosion, although the model that was used by the MPC was the plant model. The next step should be to use the data driven model as the model for the MPC. Further on, making data driven models from experiments and applying this in a model predictive control framework should be done to further validate that data driven models can be used in an MPC application to control erosion. There has already been done work to create this rig, but due to time limits for this thesis it was not able to be used. The setup consists of three different pipelines. Inside each of these pipelines, a probe is attached together with two cameras per probe. The flow through the pipelines can be controlled and it also has the possibilities of adding air and sand to the system. By using the cameras and software to measure the erosion along with a data driven model could be used in an model predictive controller to control the erosion.

Bibliography

[1] Xianghui Chen, Brenton S. McLaury, and Siamack A. Shirazi. A Comprehensive Procedure to Estimate Erosion in Elbows for Gas/Liquid/Sand Multiphase Flow. *Journal of Energy Resources Technology*, 128(1):70–78, 08 2005.

[2] Quamrul H. Mazumder, Siamack A. Shirazi, and Brenton S. McLaury. A Mechanistic Model to Predict Sand Erosion in Multiphase Flow in Elbows Downstream of Vertical Pipes. *Journal of Energy Resources Technology*, 2005.

[3] DNV-GL. Managing Sand Production and Erosion. 2015.

[4] Mazdak Parsi, Kamyar Najmi, Fardis Najafifard, Shokrollah Hassani, Brenton S. McLaury, and Siamack A. Shirazi. A comprehensive review of solid particle erosion modeling for oil and gas wells and pipelines applications. *Journal of Natural Gas Science and Engineering*, 21:850 – 873, 2014.

[5] Dinesh Krishnamoorthy, Bjarne Foss, and Sigurd Skogestad. Real-Time Optimization under Uncertainty Applied to a Gas Lifted Well Network. 2016.

[6] Lorenz T Biegler. *Nonlinear programming concepts, algorithms, and applications to chemical processes*. S.l.], 2010.

[7] Martin Behrendt. Mpc scheme basic. https://commons.wikimedia.org/w/index.php?curid=7963069. cc by-sa 3.0.

[8] John Hedengren, Reza Asgharzadeh Shishavan, Kody Powell, and Thomas Edgar. Nonlinear modeling, estimation and predictive control in apmonitor. *Computers & Chemical Engineering*, 70, 11 2014.

[9] Andreas Wächter and Lorenz Biegler. On the implementation of a primal-dual interior point filter line search algorithm for large-scale nonlinear programming. *Mathematical Programming*, 2006.

[10] Karel J. Keesman. *System Identification: An Introduction*. Springer, London, 2011.

[11] James Gareth, Trevor Hastie, Robert Tibshirani, and Daniela Witten. *An Introduction to Statistical Learning with Applications in R*. Springer, New York, 2013.

[12] J.P. Norton. *An Introduction to Identification*. Academic Press, London, 1986.

[13] Lennart Ljung. *System identification : theory for the user*. Prentice-Hall information and system sciences series. Prentice-Hall, Englewood Cliffs, N.J, 1987.

[14] Joel A E Andersson, Joris Gillis, Greg Horn, James B Rawlings, and Moritz Diehl. CasADi – A software framework for nonlinear optimization and optimal control. *Mathematical Programming Computation*, In Press, 2018.

Appendix

A Parameters for erosion modelling

Table 6: Parameters used for calculating the erosion rate.

Parameter	Explanation	Value	Unit
ρ_p	Density of sand particles	$2.5 \cdot 10^3$	$\mathrm{kg\,m^{-3}}$
C_1	Model geometry factor	1.25	-
C_{unit}	Unit conversion factor	1000	$\mathrm{mm\,m^{-1}}$
D	Length from cage and choke body	0.1	m
d_p	Sand particle diameter	$2.5 \cdot 10^{-4}$	m
GF	Geometry factor	2.0	-
H	Height of gallery	0.3	m
K	Material erosion constant	$2 \cdot 10^{-9}$	-
Mm_g	Molar mass of gas	20	$\mathrm{g\,mol^{-1}}$
$\dot{m}_p$	Sand rate	$50 \cdot 10^{-2}$	$\mathrm{kg\,s^{-1}}$
n	Velocity exponent	2.6	-
r	Radius of curvature	0.2	m

B Parameters for gas lift

Table 7: Parameters used for gas lift model.

Parameter	Explanation	Value	Unit
μ_o	Dynamic viscosity of oil	0.001	Pa s
ρ_o	Density of oil	$8 \cdot 10^2$	$\mathrm{kg\,m^{-3}}$
ρ_{ro}	Density of oil in riser	$8 \cdot 10^2$	$\mathrm{kg\,m^{-3}}$
A_r	Cross-sectional area of riser	0.0115	$\mathrm{m^2}$
C_{pr}	Valve constant for riser valve	0.01	-
D_r	Diameter of riser	0.121	m
H_r	Height of riser	500	m
L_r	Length of riser	500	m
n_w	Number of wells	3	-
p_s	Separator pressure	20	bar
T	Sampling time	86400	s
T_r	Riser temperature	303	K

Table 8: Well specific parameters used for gas lift model.

Parameter	Explanation	Well 1	Well 2	Well 3	Unit
A_{bh}	Cross-sectional area of well below injection point	0.0115	0.0115	0.0115	m^2
A_w	Cross-sectional area of well above injection point	0.0115	0.0115	0.0115	m^2
C_{iv}	Valve constant for injection valve	0.0003	0.0003	0.0003	-
C_{pc}	Valve constant for production valve	0.002	0.002	0.002	-
D_a	Diameter of annulus	0.189	0.189	0.189	m
D_{bh}	Diameter of well below injection point	0.121	0.121	0.121	m
D_w	Diameter of well above injection point	0.121	0.121	0.121	m
GOR	Gas oil ratio	0.10	0.12	0.11	-
H_a	Height of annulus	1000	1000	1000	m
H_{bh}	Height of tubing below injection point	500	500	500	m
H_w	Height of tubing above injection point	1000	1000	1000	m
L_a	Length of annulus	1500	1500	1500	m
L_{bh}	Length of pipe below injection point	500	500	500	m
L_w	Length of pipe above injection point	1500	1500	1500	m
p_r	Reservoir pressure	150	155	160	bar
PI	Reservoir productivity index	5	5	5 -	
T_a	Annulus temperature	301	301	301	K
T_w	Well temperature	305	305	305	K

C Calculation of dynamic viscosity of mixture

Under the assumption of ideal gas, the density of the gas, ρ_g, can be found as a function of the molar mass, temperature and pressure.

$$\rho_g = \frac{p_m \cdot Mm_g}{R \cdot T_w} \tag{52}$$

Where p_m is the pressure in the manifold and T_r is the temperature in the riser.

The mixed volumetric flow is the sum of the liquid volumetric flow and the gas volumetric flow.

$$Q_m = Q_{po} + Q_{pg} = \frac{w_{po}}{\rho_o} + \frac{w_{pg}}{\rho_g} \tag{53}$$

Where Q_m, Q_{po} and Q_{pg} is the mixed, oil and gas volumetric flows.

Substituting Eq. (52) into Eq. (53) gives an expression for the mixed volumetric flow:

$$Q_m = \frac{w_{po}}{\rho_o} + \frac{R \cdot T_w \cdot w_{pg}}{p_{wh} \cdot Mm_g} \tag{54}$$

The dynamic viscosity for the mixture, μ_m, is given by:

$$\mu_m = \frac{\mu_o \cdot V_o + \mu_g \cdot V_g}{V_o + V_g} \tag{55}$$

Where μ_o and μ_g are the dynamic viscosities of the oil and gas.

$V_o = \frac{Q_{po}}{A_p}$ and $V_g = \frac{Q_{pg}}{A_p}$ where V_o and V_g is the velocity of oil and gas. A_p is the pipe diameter.

$$\mu_m = \frac{\mu_o \cdot Q_{po}}{Q_{po} + Q_{pg}} + \frac{\mu_g \cdot Q_{pg}}{Q_{po} + Q_{pg}} \tag{56}$$

This is further simplified under the assumption that the viscosity of the gas, μ_g, is much lower than the viscosity of the liquid, μ_o.

$$\mu_m = \frac{\mu_o \cdot Q_{po}}{Q_{po} + Q_{pg}} \tag{57}$$

Substituting Eq. (54) into equation Eq. (57) gives:

$$\mu_m = \mu_o \cdot \frac{\frac{w_{po}}{\rho_o}}{\frac{w_{po}}{\rho_o} + \frac{R \cdot T_w \cdot w_{pg}}{p_{wh} \cdot Mm_g}} \tag{58}$$

D Least Squares Estimator

Least squares estimation is used to minimize the squared prediction error, where the prediction error can be written as $\varepsilon = y - \Phi^T \nu$ [10].

$$\begin{aligned} J(\nu) &= \varepsilon^T \cdot \varepsilon && (59)\\ &= (y - \Phi^T \nu)^T (y - \phi^T \nu) && (60)\\ &= y^T y - y^T \Phi \nu - \nu^T \Phi^T y + \nu^T \Phi^T \Phi \nu && (61)\\ &= y^T y - 2\nu^T \Phi^T y + \nu^T \Phi^T \Phi \nu && (62) \end{aligned}$$

Where $J(\nu)$ is the cost function which describes the squared prediction error. y is a vector describing observed measurements and Φ is the regressor matrix. ν describes the weightings of, for instance, an ARX model. Minimizing the cost function gives:

$$\frac{\partial J(\nu)}{\partial \nu} = 0 = -2\nu^T y + 2\Phi^T \Phi \nu \tag{63}$$

As $\Phi^T \Phi$ is a symmetric matrix, it can also be inverted. Solving Eq. (63) for the weights, νm gives the following prediction:

$$\hat{v} = (\Phi^T \Phi)^{-1} \Phi^T y \tag{64}$$